Chapter 3

Angular n-point Harmonic Spectrum on the Sky

The angular n-point correlation function,

$$\langle f(\hat{\mathbf{n}}_1) f(\hat{\mathbf{n}}_2) \dots f(\hat{\mathbf{n}}_n) \rangle , \tag{3.1}$$

is a simple statistic characterizing a clustering pattern of fluctuations on the sky, $f(\hat{\mathbf{n}})$. Here, the bracket denotes the ensemble average, and figure 3.1 sketches the meaning. If the fluctuation is Gaussian, then the two-point correlation function specifies all the statistical properties of $f(\hat{\mathbf{n}})$, for the two-point correlation function is the only parameter in Gaussian distribution. If it is not Gaussian, then we need higher-order correlation functions to determine the statistical properties.

Yet simple, one disadvantage of the angular correlation function is that data points of the correlation function at different angular scales are generally not independent of each other, but correlated: two-point correlation at 1 degree is correlated with that at 2 degrees, and so on. This property makes a detailed statistical analysis and interpretation of the data complicated.

Hence, one finds it more convenient to expand $f(\hat{\mathbf{n}})$ into spherical harmonics, the orthonormal basis on the sphere, as

$$f(\hat{\mathbf{n}}) = \sum_{l=0}^{\infty} \sum_{m=-l}^{l} a_{lm} Y_{lm}(\hat{\mathbf{n}}), \tag{3.2}$$

and then to consider the angular n-point harmonic spectrum, $\langle a_{l_1 m_1} a_{l_2 m_2} \dots a_{l_n m_n} \rangle$. While a_{lm} for $m \neq 0$ is complex, reality of $f(\hat{\mathbf{n}})$ gives $a_{l-m} = a_{lm}^*(-1)^m$, and thus the number of independent modes is not $4l+1$, but $2l+1$.

Especially, the angular two-, three-, and four-point harmonic spectra are called the angular *power spectrum*, *bispectrum*, and *trispectrum*, respectively. For a Gaussian field, the angular spectra at different angular scales, or at different l's, are uncorrelated. Even for a non-Gaussian field, they are reasonably uncorrelated as long as the non-Gaussianity is weak. Moreover, since the spherical harmonic is orthogonal for different l's, it highlights characteristic structures on the sky at a given l. In other words, even if the angular correlation function is featureless, the angular spectrum may

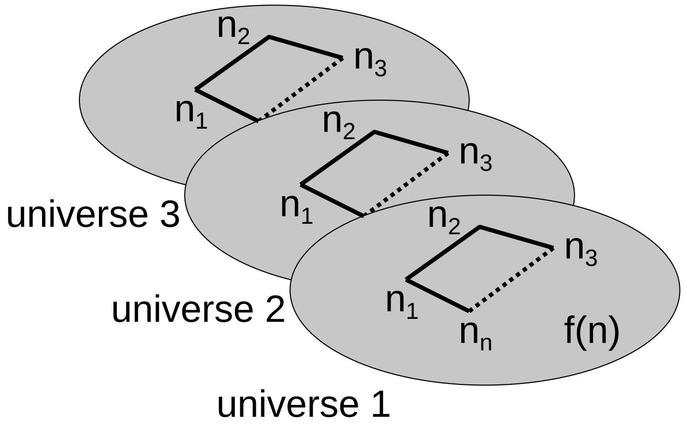

Figure 3.1: Ensemble Average of Angular Correlation Function

A schematic view of the ensemble average of the n-point angular correlation function, $f(\hat{\mathbf{n}}_1)f(\hat{\mathbf{n}}_2)f(\hat{\mathbf{n}}_3)\dots f(\hat{\mathbf{n}}_n)$. We measure it on each universe, and then average it over many universes.

have a distinct structure, for inflation predicts a prominent peak in the angular power spectrum, not in the angular correlation function. In this chapter, we study statistical properties of the angular n-point harmonic spectra.

3.1 Statistical Isotropy of the Universe

In reality, we cannot measure the ensemble average of the angular harmonic spectrum, but one realization such as $a_{l_1m_1}a_{l_2m_2}\dots a_{l_nm_n}$, which is so noisy that we want to average it somehow to reduce the noise.

We assume *statistical isotropy* of the universe from which it follows that our sky is isotropic and has no preferred direction. Isotropy of CMB justifies the assumption. The assumption readily implies that one can average the spectrum over m_i with an appropriate weight, as m_i represent an azimuthal orientation on the sky. The average over m_i enables us to reduce statistical error of the measured harmonic spectra.

How can we find the weight? One finds it as a solution to statistical isotropy, or *rotational invariance* of the angular correlation function on the sky,

$$\langle Df(\hat{\mathbf{n}}_1)Df(\hat{\mathbf{n}}_2)\dots Df(\hat{\mathbf{n}}_n)\rangle = \langle f(\hat{\mathbf{n}}_1)f(\hat{\mathbf{n}}_2)\dots f(\hat{\mathbf{n}}_n)\rangle\,, \tag{3.3}$$

where $D = D(\alpha,\beta,\gamma)$ is a rotation matrix for the Euler angles α, β, and γ. Figure 3.2 sketches the meaning of statistical isotropy. Substituting equation (3.2) for $f(\hat{\mathbf{n}})$ in equation (3.3), we then need rotation of the spherical harmonic, $DY_{lm}(\hat{\mathbf{n}})$. It is formally represented by the rotation matrix

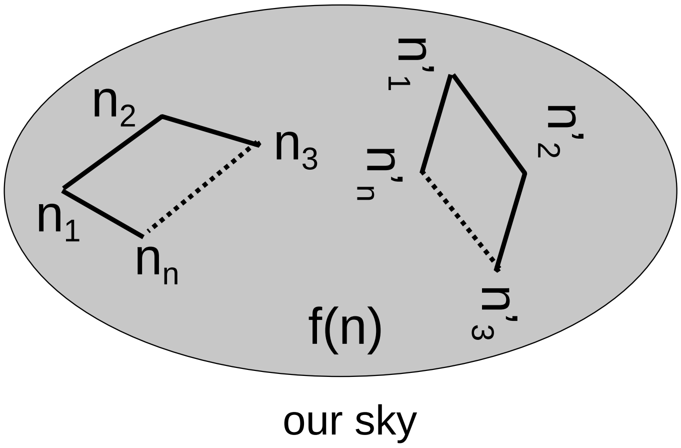

Figure 3.2: Statistical Isotropy of Angular Correlation Function

A schematic view of statistical isotropy of the angular correlation function. As long as its configuration is preserved, we can average $f(\hat{\mathbf{n}}_1)\dots f(\hat{\mathbf{n}}_n)$ over all possible orientations and positions on the sky.

element, $D^{(l)}_{m'm}(\alpha,\beta,\gamma)$, as (Rotenberg et al., 1959)

$$DY_{lm}(\hat{\mathbf{n}}) = \sum_{m'=-l}^{l} D^{(l)}_{m'm} Y_{lm'}(\hat{\mathbf{n}}). \tag{3.4}$$

The matrix element, $D^{(l)}_{m'm} = \langle l, m' | D | l, m \rangle$, describes finite rotation of an initial state whose orbital angular momentum is represented by l and m into a final state represented by l and m'. Finally, we obtain the statistical isotropy condition on the angular n-point harmonic spectrum:

$$\langle a_{l_1m_1} a_{l_2m_2} \dots a_{l_nm_n} \rangle = \sum_{\text{all } m'} \left\langle a_{l_1m_1'} a_{l_2m_2'} \dots a_{l_nm_n'} \right\rangle D^{(l_1)}_{m_1'm_1} D^{(l_2)}_{m_2'm_2} \dots D^{(l_n)}_{m_n'm_n}. \tag{3.5}$$

Using this equation, Hu (2001) has systematically evaluated appropriate weights for averaging the angular power spectrum ($n = 2$), bispectrum ($n = 3$), and trispectrum ($n = 4$), over azimuthal angles. Some of those may be found more intuitively; however, this method allows us to find the weight for any higher-order harmonic spectrum. In the following sections, we derive rotationally invariant, azimuthally averaged harmonic spectra for $n = 2$, 3, and 4, and study their statistical properties.

3.2 Angular Power Spectrum

The angular power spectrum measures how much fluctuations exist on a given angular scale. For example, the variance of a_{lm} for $l \geq 1$, $\langle a_{lm} a^*_{lm} \rangle$, measures the amplitude of fluctuations at a given l.

Generally speaking, the covariance matrix of a_{lm}, $\left\langle a_{l_1m_1}a^*_{l_2m_2}\right\rangle$, is not necessarily diagonal. It is, however, actually diagonal once we assume full sky coverage and rotational invariance of the angular two-point correlation function, as we will show in this section. The variance of a_{lm} thus describes the two-point correlation completely.

Rotational invariance (Eq.(3.5)) requires

$$\langle a_{l_1m_1}a^*_{l_2m_2}\rangle = \sum_{m_1'm_2'} \left\langle a_{l_1m_1'}a^*_{l_2m_2'}\right\rangle D^{(l_1)}_{m_1'm_1} D^{(l_2)*}_{m_2'm_2} \tag{3.6}$$

to be satisfied, where we have used the complex conjugate for simplifying calculations. From this equation, we seek for a rotationally invariant representation of the angular power spectrum. Suppose that the covariance matrix of a_{lm} is diagonal, i.e., $\left\langle a_{l_1m_1}a^*_{l_2m_2}\right\rangle = \langle C_{l_1}\rangle \delta_{l_1l_2}\delta_{m_1m_2}$. Equation (3.6) then reduces to

$$\langle a_{l_1m_1}a^*_{l_2m_2}\rangle = \langle C_{l_1}\rangle \delta_{l_1l_2} \sum_{m_1'} D^{(l_1)}_{m_1'm_1} D^{(l_1)*}_{m_1'm_2} = \langle C_{l_1}\rangle \delta_{l_1l_2}\delta_{m_1m_2}. \tag{3.7}$$

Thus, we have proven $\langle C_l\rangle$ rotationally invariant. Rotational invariance implies that the covariance matrix is diagonal.

3.2.1 Estimator

Observationally, the unbiased estimator of $\langle C_l\rangle$ should be

$$\begin{aligned} C_l &= \frac{1}{2l+1}\sum_{m=-l}^{l} a_{lm}a^*_{lm} = \frac{1}{2l+1}\left(a^2_{l0} + 2\sum_{m=1}^{l} a_{lm}a^*_{lm}\right) \\ &= \frac{1}{2l+1}\left\{a^2_{l0} + 2\sum_{m=1}^{l}\left[(\Re a_{lm})^2 + (\Im a_{lm})^2\right]\right\}. \end{aligned} \tag{3.8}$$

The second equality follows from $a_{l-m} = a^*_{lm}(-1)^m$, i.e., $a_{l-m}a^*_{l-m} = a_{lm}a^*_{lm}$, and hence we average $2l+1$ independent samples for a given l. It suggests that fractional statistical error of C_l is reduced by $\sqrt{1/(2l+1)}$. This property is the main motivation of our considering the azimuthally averaged harmonic spectrum.

We find it useful to define an azimuthally averaged harmonic transform, $e_l(\hat{\mathbf{n}})$, as

$$e_l(\hat{\mathbf{n}}) \equiv \sqrt{\frac{4\pi}{2l+1}}\sum_{m=-l}^{l} a_{lm}Y_{lm}(\hat{\mathbf{n}}), \tag{3.9}$$

which is interpreted as a square-root of C_l at a given position of the sky,

$$\int \frac{d^2\hat{\mathbf{n}}}{4\pi}\, e^2_l(\hat{\mathbf{n}}) = C_l. \tag{3.10}$$

$e_l(\hat{\mathbf{n}})$ is particularly useful for measuring the angular bispectrum (Spergel and Goldberg, 1999; Komatsu et al., 2001b) (chapter 5), trispectrum (chapter 6), and probably any higher-order harmonic spectra, because of being computationally very fast to calculate. This is very important, as the new satellite experiments, *MAP* and *Planck*, have more than millions of pixels, for which we will crucially need a fast algorithm of measuring these higher-order harmonic spectra.

3.2.2 Covariance matrix

We derive the covariance matrix of C_l, $\langle C_l C_{l'}\rangle - \langle C_l\rangle\langle C_{l'}\rangle$, with the four-point function, the trispectrum. Starting with

$$\langle C_l C_{l'}\rangle = \frac{1}{(2l+1)(2l'+1)}\sum_{mm'}\langle a_{lm}a^*_{lm}a_{l'm'}a^*_{l'm'}\rangle\,, \tag{3.11}$$

we obtain the power spectrum covariance matrix

$$\begin{aligned}\langle C_l C_{l'}\rangle - \langle C_l\rangle\langle C_{l'}\rangle &= \frac{2\langle C_l\rangle^2}{2l+1}\delta_{ll'} + \frac{1}{(2l+1)(2l'+1)}\sum_{mm'}\langle a_{lm}a^*_{lm}a_{l'm'}a^*_{l'm'}\rangle_{\rm c} \\ &= \frac{2\langle C_l\rangle^2}{2l+1}\delta_{ll'} + \frac{(-1)^{l+l'}}{\sqrt{(2l+1)(2l'+1)}}\left\langle T^{ll}_{l'l'}(0)\right\rangle_{\rm c}\,, \end{aligned}\tag{3.12}$$

where $\langle a_{lm}a^*_{lm}a_{l'm'}a^*_{l'm'}\rangle_{\rm c}$ is the connected four-point harmonic spectrum, the connected trispectrum, which is exactly zero for a Gaussian field. It follows from this equation that the covariance matrix of C_l is exactly diagonal only when a_{lm} is Gaussian. $\left\langle T^{l_1l_2}_{l_3l_4}(L)\right\rangle_{\rm c}$ is the ensemble average of the angular averaged connected trispectrum, which we will define in § 3.4 (Eq.(3.24)).

Unfortunately, we cannot measure the connected $T^{ll}_{l'l'}(0)$ directly from the angular trispectrum (see § 3.4). We will thus never be sure if the power spectrum covariance is precisely diagonal, as long as we use the angular trispectrum. We need the other statistics that can pick up information of the connected $T^{ll}_{l'l'}(0)$, even though they are indirect. Otherwise, we need a model for the connected trispectrum, and use the model to constrain the connected $T^{ll}_{l'l'}(0)$ from the other trispectrum configurations. We will discuss this point in chapter 6.

There is no reason to assume the connected $T^{ll}_{l'l'}(0)$ small. It is produced on large angular scales, if topology of the universe is closed hyperbolic (Inoue, 2001b). In appendix D, we derive an analytic prediction for the connected trispectrum produced in a closed hyperbolic universe. On small angular scales, several authors have shown that the weak gravitational lensing effect produces the connected trispectrum or four-point correlation function (Bernardeau, 1997; Zaldarriaga and Seljak, 1999; Zaldarriaga, 2000); Hu (2001) finds that the induced off-diagonal terms are negligible compared with the diagonal terms out to $l \sim 2000$.

If the connected trispectrum is negligible, then we obtain

$$\langle C_l C_{l'}\rangle - \langle C_l\rangle\langle C_{l'}\rangle \approx \frac{2\langle C_l\rangle^2}{2l+1}\delta_{ll'}. \tag{3.13}$$

The fractional error of C_l is thus proportional to $\sqrt{1/(2l+1)}$, as expected from our having $2l+1$ independent samples to average for a given l. The exact form follows from C_l being χ^2 distribution with $2l+1$ degrees of freedom when a_{lm} is Gaussian. If a_{lm} is Gaussian, then its probability density distribution is

$$P\left(a_{lm}\right) = \frac{\exp\left[-a^2_{lm}/(2\langle C_l\rangle)\right]}{\sqrt{2\pi\langle C_l\rangle}}. \tag{3.14}$$

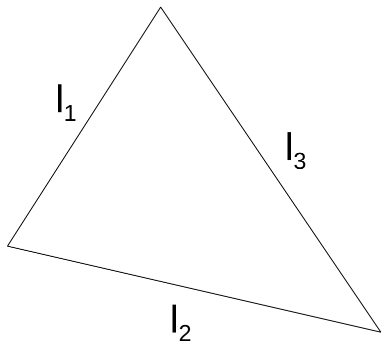

Figure 3.3: Angular Bispectrum Configuration

We use this distribution to generate Gaussian random realizations of a_{lm} for a given $\langle C_l \rangle$. First, we calculate $\langle C_l \rangle$ with the CMBFAST code (Seljak and Zaldarriaga, 1996) for a set of cosmological parameters. We then generate a realization of a_{lm}, $a_{lm} = \epsilon \langle C_l \rangle^{1/2}$, where ϵ is a Gaussian random variable with the unit variance.

3.3 Angular Bispectrum

The angular bispectrum consists of three harmonic transforms, $a_{l_1m_1}a_{l_2m_2}a_{l_3m_3}$. For Gaussian a_{lm}, the expectation value is exactly zero. By imposing statistical isotropy upon the angular three-point correlation function, one finds that the angular averaged bispectrum, $B_{l_1l_2l_3}$, given by

$$\langle a_{l_1m_1}a_{l_2m_2}a_{l_3m_3} \rangle = \langle B_{l_1l_2l_3} \rangle \begin{pmatrix} l_1 & l_2 & l_3 \\ m_1 & m_2 & m_3 \end{pmatrix} \tag{3.15}$$

satisfies rotational invariance (Eq.(3.5)). Here, the matrix denotes the Wigner-$3j$ symbol (see appendix B). Since l_1, l_2, and l_3 form a triangle, $B_{l_1l_2l_3}$ satisfies the triangle condition, $|l_i - l_j| \leq l_k \leq l_i + l_j$ for all permutations of indices. Parity invariance of the angular correlation function demands $l_1 + l_2 + l_3 =$ even. Figure 3.3 sketches a configuration of the angular bispectrum.

The Wigner-$3j$ symbol, which describes coupling of two angular momenta, represents the azimuthal angle dependence of the angular bispectrum, for the bispectrum forms a triangle. Suppose that two "states" with (l_1, m_1) and (l_2, m_2) angular momenta form a coupled state with (l_3, m_3). They form a triangle whose orientation is represented by m_1, m_2, and m_3, with satisfying $m_1 + m_2 + m_3 = 0$. As we rotate the system, the Wigner-$3j$ symbol transforms m's, yet preserving the configuration of the triangle. Similarly, rotational invariance of the angular bispectrum demands that the same triangle configuration give the same amplitude of the bispectrum regardless of its orientation, and thus the Wigner-$3j$ symbol describes the azimuthal angle dependence.

The proof of $\langle B_{l_1l_2l_3} \rangle$ to be rotationally invariant is as follows. Substituting equation (3.15) for the statistical isotropy condition (Eq.(3.5)) for $n = 3$, we obtain

$$\langle a_{l_1m_1}a_{l_2m_2}a_{l_3m_3} \rangle$$

$$
\begin{aligned}
&= \sum_{\text{all } m'} \left\langle a_{l_1m_1'} a_{l_2m_2'} a_{l_3m_3'} \right\rangle D^{(l_1)}_{m_1'm_1} D^{(l_2)}_{m_2'm_2} D^{(l_3)}_{m_3'm_3} \\
&= \langle B_{l_1l_2l_3} \rangle \sum_{\text{all } m'} \begin{pmatrix} l_1 & l_2 & l_3 \\ m_1' & m_2' & m_3' \end{pmatrix} \\
&\quad \times \sum_{LMM'} \begin{pmatrix} l_1 & l_2 & L \\ m_1' & m_2' & M' \end{pmatrix} \begin{pmatrix} l_1 & l_2 & L \\ m_1 & m_2 & M \end{pmatrix} (2L+1) D^{(L)*}_{M'M} D^{(l_3)}_{m_3'm_3} \\
&= \langle B_{l_1l_2l_3} \rangle \sum_{m_3'} \sum_{LMM'} \delta_{l_3L} \delta_{m_3'M'} \begin{pmatrix} l_1 & l_2 & L \\ m_1 & m_2 & M \end{pmatrix} D^{(L)*}_{M'M} D^{(l_3)}_{m_3'm_3} \\
&= \langle B_{l_1l_2l_3} \rangle \begin{pmatrix} l_1 & l_2 & l_3 \\ m_1 & m_2 & m_3 \end{pmatrix}. \qquad (3.16)
\end{aligned}
$$

In the second equality, we have reduced $D^{(l_1)}_{m_1'm_1} D^{(l_2)}_{m_2'm_2}$ to $D^{(L)*}_{M'M}$, using equation (B.17). In the third equality, we have used the identity (Rotenberg et al., 1959),

$$
\sum_{m_1'm_2'} \begin{pmatrix} l_1 & l_2 & l_3 \\ m_1' & m_2' & m_3' \end{pmatrix} \begin{pmatrix} l_1 & l_2 & L \\ m_1' & m_2' & M' \end{pmatrix} = \frac{\delta_{l_3L}\delta_{m_3'M'}}{2L+1}. \qquad (3.17)
$$

3.3.1 Estimator

To obtain the unbiased estimator of the angular averaged bispectrum, $B_{l_1l_2l_3}$, we invert equation (3.15) with the identity (3.17), and obtain

$$
B_{l_1l_2l_3} = \sum_{\text{all } m} \begin{pmatrix} l_1 & l_2 & l_3 \\ m_1 & m_2 & m_3 \end{pmatrix} a_{l_1m_1} a_{l_2m_2} a_{l_3m_3}. \qquad (3.18)
$$

We can rewrite this expression into a more computationally useful form. Using the azimuthally averaged harmonic transform, $e_l(\hat{\mathbf{n}})$ (Eq.(3.9)), and the identity (Rotenberg et al., 1959),

$$
\begin{aligned}
\begin{pmatrix} l_1 & l_2 & l_3 \\ m_1 & m_2 & m_3 \end{pmatrix} &= \begin{pmatrix} l_1 & l_2 & l_3 \\ 0 & 0 & 0 \end{pmatrix}^{-1} \sqrt{\frac{(4\pi)^3}{(2l_1+1)(2l_2+1)(2l_3+1)}} \\
&\quad \times \int \frac{d^2\hat{\mathbf{n}}}{4\pi} Y_{l_1m_1}(\hat{\mathbf{n}}) Y_{l_2m_2}(\hat{\mathbf{n}}) Y_{l_3m_3}(\hat{\mathbf{n}}), \qquad (3.19)
\end{aligned}
$$

we rewrite equation (3.18) as

$$
B_{l_1l_2l_3} = \begin{pmatrix} l_1 & l_2 & l_3 \\ 0 & 0 & 0 \end{pmatrix}^{-1} \int \frac{d^2\hat{\mathbf{n}}}{4\pi} e_{l_1}(\hat{\mathbf{n}}) e_{l_2}(\hat{\mathbf{n}}) e_{l_3}(\hat{\mathbf{n}}). \qquad (3.20)
$$

This expression is computationally efficient; we can quickly calculate $e_l(\hat{\mathbf{n}})$ with the spherical harmonic transform. Then, the average over the full sky, $\int d^2\hat{\mathbf{n}}/(4\pi)$, is done by the sum over all pixels divided by the total number of pixels, $N^{-1}\sum_i^N$, if all the pixels have the equal area. Note that the integral over $\hat{\mathbf{n}}$ must be done on the full sky even when a sky-cut is applied, as $e_l(\hat{\mathbf{n}})$ already encapsulates information of partial sky coverage through a_{lm}, which may be measured on the incomplete sky.

3.3.2 Covariance matrix

We calculate the covariance matrix of $B_{l_1l_2l_3}$, provided that non-Gaussianity is weak, $\langle B_{l_1l_2l_3}\rangle \approx 0$. Since the covariance matrix is a product of six a_{lm}'s, we have ${}_6C_2 \cdot {}_4C_2/3! = 15$ terms to evaluate, according to the Wick's theorem; however, using the identity (Rotenberg et al., 1959),

$$(-1)^m \begin{pmatrix} l & l & l' \\ m & -m & 0 \end{pmatrix} = \frac{(-1)^l}{\sqrt{2l+1}}\delta_{l'0}, \tag{3.21}$$

and assuming none of l's zero, we find only $3! = 6$ terms that do not include $\left\langle a_{l_im_i}a_{l_jm_j}\right\rangle$ but include only $\left\langle a_{l_im_i}a^*_{l_jm_j}\right\rangle$ non-vanishing. Evaluating these 6 terms, we obtain (Luo, 1994; Heavens, 1998; Spergel and Goldberg, 1999; Gangui and Martin, 2000)

$$\begin{aligned}
&\left\langle B_{l_1l_2l_3}B_{l_1'l_2'l_3'}\right\rangle \\
&= \sum_{\text{all } mm'} \begin{pmatrix} l_1 & l_2 & l_3 \\ m_1 & m_2 & m_3 \end{pmatrix}\begin{pmatrix} l_1' & l_2' & l_3' \\ m_1' & m_2' & m_3' \end{pmatrix}\left\langle a_{l_1m_1}a_{l_2m_2}a_{l_3m_3}a^*_{l_1'm_1'}a^*_{l_2'm_2'}a^*_{l_3'm_3'}\right\rangle \\
&= \langle C_{l_1}\rangle\langle C_{l_2}\rangle\langle C_{l_3}\rangle\left[\delta^{l_1'l_2'l_3'}_{l_1l_2l_3} + \delta^{l_3'l_1'l_2'}_{l_1l_2l_3} + \delta^{l_2'l_3'l_1'}_{l_1l_2l_3} + (-1)^{l_1+l_2+l_3}\left(\delta^{l_1'l_3'l_2'}_{l_1l_2l_3} + \delta^{l_2'l_1'l_3'}_{l_1l_2l_3} + \delta^{l_3'l_2'l_1'}_{l_1l_2l_3}\right)\right],
\end{aligned} \tag{3.22}$$

where $\delta^{l_1'l_2'l_3'}_{l_1l_2l_3} \equiv \delta_{l_1l_1'}\delta_{l_2l_2'}\delta_{l_3l_3'}$, and so on. Hence, the covariance matrix is diagonal in the weak non-Gaussian limit. The diagonal terms for $l_i \neq 0$ and $l_1 + l_2 + l_3 =$ even are

$$\left\langle B^2_{l_1l_2l_3}\right\rangle = \langle C_{l_1}\rangle\langle C_{l_2}\rangle\langle C_{l_3}\rangle\left(1 + 2\delta_{l_1l_2}\delta_{l_2l_3} + \delta_{l_1l_2} + \delta_{l_2l_3} + \delta_{l_3l_1}\right). \tag{3.23}$$

The variance is amplified by a factor of 2 or 6, when two or all l's are same, respectively.

We find that equation (3.23) becomes not exact on the incomplete sky, where the variance distribution becomes more scattered. Using simulated realizations of a Gaussian sky, we have measured the variance on the full sky as well as on the incomplete sky for three different Galactic sky-cuts, 20°, 25°, and 30°. Figure 3.4 plots the results; we find that equation (3.23) holds only approximately on the incomplete sky.

3.4 Angular Trispectrum

The angular trispectrum consists of four harmonic transforms, $a_{l_1m_1}a_{l_2m_2}a_{l_3m_3}a_{l_4m_4}$. Hu (2001) finds a rotationally invariant solution for the angular trispectrum as

$$\langle a_{l_1m_1}a_{l_2m_2}a_{l_3m_3}a_{l_4m_4}\rangle = \sum_{LM}\begin{pmatrix} l_1 & l_2 & L \\ m_1 & m_2 & -M \end{pmatrix}\begin{pmatrix} l_3 & l_4 & L \\ m_3 & m_4 & M \end{pmatrix}(-1)^M\left\langle T^{l_1l_2}_{l_3l_4}(L)\right\rangle. \tag{3.24}$$

One can prove this solution, $\left\langle T^{l_1l_2}_{l_3l_4}(L)\right\rangle$, rotationally invariant by similar calculations to those proving the angular bispectrum to be so. By construction, l_1, l_2, and L form one triangle, while l_3, l_4, and L form the other triangle in a quadrilateral with sides of l_1, l_2, l_3, and l_4. L represents

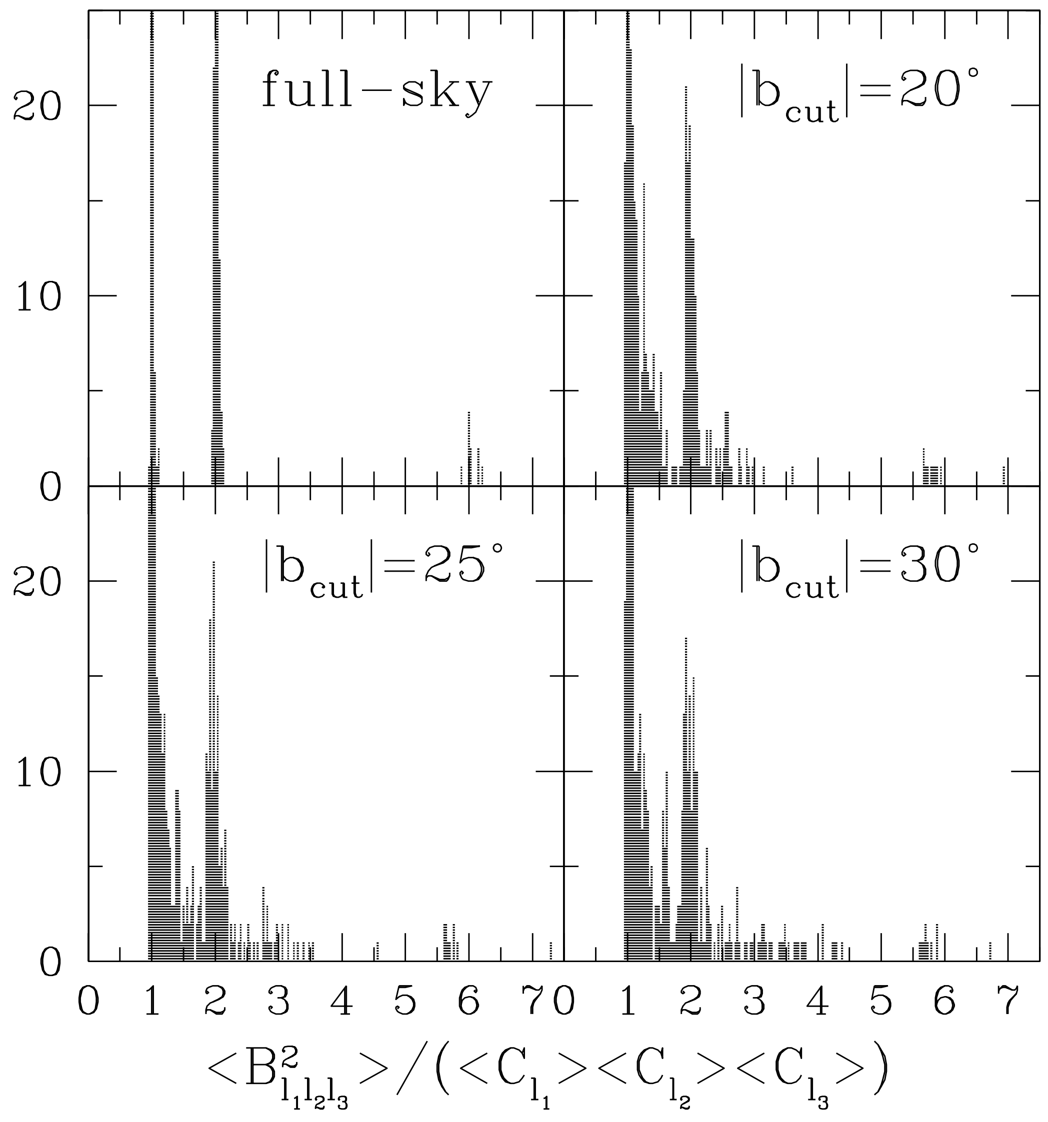

Figure 3.4: Variance of Angular Bispectrum

Histograms of variance of the angular bispectrum for $l_1 \leq l_2 \leq l_3$ up to a maximum multipole of 20. There are 466 modes. These are derived from simulated realizations of a Gaussian sky. The top-left panel shows the case of full sky coverage, while the rest of panels show the cases of incomplete sky coverage. The top-right, bottom-left, and bottom-right panels use the 20°, 25°, and 30° Galactic sky-cuts, respectively.

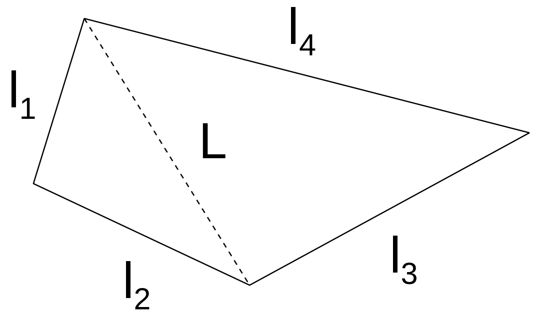

Figure 3.5: Angular Trispectrum Configuration

a diagonal of the quadrilateral. Figure 3.5 sketches a configuration of the angular trispectrum. When we arrange l_1, l_2, l_3, and l_4 in order of $l_1 \le l_2 \le l_3 \le l_4$, L lies in $\max(l_2 - l_1, l_4 - l_3) \le L \le \min(l_1 + l_2, l_3 + l_4)$. Parity invariance of the angular four-point correlation function demands $l_1 + l_2 + L =$ even and $l_3 + l_4 + L =$ even.

The angular trispectrum generically consists of two parts. One is the unconnected part, the contribution from Gaussian fields, which is given by the angular power spectra (Hu, 2001),

$$\begin{aligned} & \left\langle T^{l_1 l_2}_{l_3 l_4}(L) \right\rangle_{\text{unconnected}} \\ = \; & (-1)^{l_1+l_3}\sqrt{(2l_1+1)(2l_3+1)}\,\langle C_{l_1}\rangle \langle C_{l_3}\rangle \delta_{l_1 l_2}\delta_{l_3 l_4}\delta_{L0} \\ & +(2L+1)\langle C_{l_1}\rangle \langle C_{l_2}\rangle \left[(-1)^{l_2+l_3+L}\delta_{l_1 l_3}\delta_{l_2 l_4} + \delta_{l_1 l_4}\delta_{l_2 l_3}\right]. \end{aligned} \tag{3.25}$$

For $l_1 \le l_2 \le l_3 \le l_4$, the unconnected terms are non-zero only when $L = 0$ or $l_1 = l_2 = l_3 = l_4$. We have numerically confirmed that our estimator given below (Eq.(3.30)) accurately reproduces the unconnected terms (Eq.(3.25)) on a simulated Gaussian sky.

The other is the connected part whose expectation value is exactly zero for Gaussian fields; thus, the connected part is sensitive to non-Gaussianity. When none of l's are same in $T^{l_1 l_2}_{l_3 l_4}(L)$, one might expect the trispectrum to comprise the connected part only; however, it is true only on the full sky. The unconnected terms on the incomplete sky, which are often much bigger than the connected terms, leak the power to the other modes for which all l's are different. We should take this effect into account in the analysis.

3.4.1 Estimator

Inverting equation (3.24), we obtain the unbiased estimator of $T^{l_1 l_2}_{l_3 l_4}(L)$ (Hu, 2001),

$$\begin{aligned} T^{l_1 l_2}_{l_3 l_4}(L) = \; & (2L+1)\sum_{\text{all } m}\sum_{M}(-1)^M \begin{pmatrix} l_1 & l_2 & L \\ m_1 & m_2 & M \end{pmatrix} \begin{pmatrix} l_3 & l_4 & L \\ m_3 & m_4 & -M \end{pmatrix} \\ & \times a_{l_1 m_1} a_{l_2 m_2} a_{l_3 m_3} a_{l_4 m_4}. \end{aligned} \tag{3.26}$$

Note that this expression includes both the connected and the unconnected terms.

We find that this estimator has a special property for $L = 0$ (which demands $l_1 = l_2$ and $l_3 = l_4$). The trispectrum estimator for these configurations, $T^{l_1 l_1}_{l_3 l_3}(0)$, reduces to a product of two power spectrum estimators, $C_{l_1} C_{l_3}$,

$$\begin{aligned} T^{l_1 l_1}_{l_3 l_3}(0) &= \sum_{m_1 m_3} \begin{pmatrix} l_1 & l_1 & 0 \\ m_1 & -m_1 & 0 \end{pmatrix} \begin{pmatrix} l_3 & l_3 & 0 \\ m_3 & -m_3 & 0 \end{pmatrix} a_{l_1 m_1} a_{l_1 -m_1} a_{l_3 m_3} a_{l_3 -m_3} \\ &= (-1)^{l_1+l_3} \sqrt{(2l_1+1)(2l_3+1)} C_{l_1} C_{l_3}, \end{aligned} \tag{3.27}$$

where $C_l = (2l+1)^{-1} \sum_m a_{lm} a^*_{lm}$. We have used the identity, equation (3.21), and $a_{l-m} = (-1)^m a^*_{lm}$ in the second equality. From this equation, one may assume that $T^{l_1 l_1}_{l_3 l_3}(0)$ coincides with the unconnected terms for $L = 0$ (see Eq.(3.25)),

$$\left\langle T^{l_1 l_1}_{l_3 l_3}(0) \right\rangle_{\text{unconnected}} = (-1)^{l_1+l_3} \sqrt{(2l_1+1)(2l_3+1)} \left\langle C_{l_1} \right\rangle \left\langle C_{l_3} \right\rangle + 2 \left\langle C_{l_1} \right\rangle^2 \delta_{l_1 l_3}. \tag{3.28}$$

They are, however, different for non-Gaussian fields, because of the power spectrum covariance, equation (3.12). By taking the ensemble average of $T^{l_1 l_1}_{l_3 l_3}(0)$, and substituting equation (3.12) for $\langle C_{l_1} C_{l_3} \rangle$, we find a rather trivial result:

$$\begin{aligned} \left\langle T^{l_1 l_1}_{l_3 l_3}(0) \right\rangle &= (-1)^{l_1+l_3} \sqrt{(2l_1+1)(2l_3+1)} \left\langle C_{l_1} C_{l_3} \right\rangle \\ &= (-1)^{l_1+l_3} \sqrt{(2l_1+1)(2l_3+1)} \left\langle C_{l_1} \right\rangle \left\langle C_{l_3} \right\rangle + 2 \left\langle C_{l_1} \right\rangle^2 \delta_{l_1 l_3} + \left\langle T^{l_1 l_1}_{l_3 l_3}(0) \right\rangle_{\text{c}} \\ &= \left\langle T^{l_1 l_1}_{l_3 l_3}(0) \right\rangle_{\text{unconnected}} + \left\langle T^{l_1 l_1}_{l_3 l_3}(0) \right\rangle_{\text{c}}. \end{aligned} \tag{3.29}$$

Hence, $T^{l_1 l_1}_{l_3 l_3}(0)$ contains information not only of the unconnected trispectrum, but also of the connected trispectrum.

Unfortunately, we cannot measure the connected part of $T^{l_1 l_1}_{l_3 l_3}(0)$ directly from the angular trispectrum because of the following reason. To measure the connected terms, we have to subtract the unconnected terms from the measured trispectrum first. Since we are never able to measure the ensemble average of the unconnected terms (Eq.(3.28)), we estimate them by using estimated power spectrum, C_l. If we subtract the estimated unconnected terms, $\propto C_{l_1} C_{l_3}$, from measured $T^{l_1 l_1}_{l_3 l_3}(0)$, then it follows from equation (3.27) that $T^{l_1 l_1}_{l_3 l_3}(0)$ vanishes *exactly*: $T^{l_1 l_1}_{l_3 l_3}(0) = 0$; thus, $T^{l_1 l_1}_{l_3 l_3}(0)$ has no statistical power of measuring the connected terms.

For practical measurement of the angular trispectrum, we rewrite the trispectrum estimator given by equation (3.26) with the azimuthally averaged harmonic transform, $e_l(\hat{\mathbf{n}})$ (Eq.(3.9)). We find that the following form is particularly computationally efficient:

$$T^{l_1 l_2}_{l_3 l_4}(L) = \frac{1}{2L+1} \sum_{M=-L}^{L} t^{l_1 l_2 *}_{LM} t^{l_3 l_4}_{LM}, \tag{3.30}$$

where $t^{l_1 l_2}_{LM}$ is given by

$$t^{l_1 l_2}_{LM} \equiv \sqrt{\frac{2L+1}{4\pi}} \begin{pmatrix} l_1 & l_2 & L \\ 0 & 0 & 0 \end{pmatrix}^{-1} \int d^2\hat{\mathbf{n}} \left[e_{l_1}(\hat{\mathbf{n}}) e_{l_2}(\hat{\mathbf{n}}) \right] Y^*_{LM}(\hat{\mathbf{n}}). \tag{3.31}$$

Since $t_{LM}^{l_1 l_2}$ is the harmonic transform on the full sky, we can calculate it quickly. This method makes measurement of the angular trispectrum computationally feasible even for the *MAP* data in which we have more than millions of pixels; thus, the methods developed here can be applied not only to the *COBE* DMR data, but also to the *MAP* data.

3.4.2 Covariance matrix

We calculate the covariance of the trispectrum in the weakly non-Gaussian limit. Since the trispectrum covariance comprises eight a_{lm}'s, the total number of terms is ${}_8C_2 \cdot {}_6C_2 \cdot {}_4C_2/4! = 105$ according to the Wick's theorem. The full calculation will be a nightmare, for we have to deal with

$$\begin{aligned}
&\left\langle T_{l_3 l_4}^{l_1 l_2}(L) T_{l_3' l_4'}^{l_1' l_2'}(L') \right\rangle \\
=\ & (2L+1)(2L'+1) \sum_{\text{all } mm'} \sum_{MM'} (-1)^{M+M'} \\
&\times \begin{pmatrix} l_1 & l_2 & L \\ m_1 & m_2 & M \end{pmatrix} \begin{pmatrix} l_3 & l_4 & L \\ m_3 & m_4 & -M \end{pmatrix} \begin{pmatrix} l_1' & l_2' & L' \\ m_1' & m_2' & M' \end{pmatrix} \begin{pmatrix} l_3' & l_4' & L' \\ m_3' & m_4' & -M' \end{pmatrix} \\
&\times \left\langle a_{l_1 m_1} a_{l_2 m_2} a_{l_3 m_3} a_{l_4 m_4} a_{l_1' m_1'}^* a_{l_2' m_2'}^* a_{l_3' m_3'}^* a_{l_4' m_4'}^* \right\rangle . \qquad (3.32)
\end{aligned}$$

We reduce this intricate expression to much more simplified forms for some particular configurations. For $L, L' \neq 0$ terms, thanks to the identity (3.21), only $4! = 24$ terms that do not include $\left\langle a_{l_i m_i} a_{l_j m_j} \right\rangle$ but include only $\left\langle a_{l_i m_i} a_{l_j m_j}^* \right\rangle$ are non-vanishing. For $L = L' = 0$ terms, the triangle conditions in a quadrilateral demand $l_1 = l_2$ and $l_3 = l_4$ (see figure 3.5). As we have shown, these configurations have no statistical power of measuring the connected trispectrum of interest. Hence, we evaluate $L, L' \neq 0$ terms in the following.

Evaluating 24 $L, L' \neq 0$ terms is still a headache; however, for $l_1 \le l_2 < l_3 \le l_4$, we have only 8 terms left:

$$\begin{aligned}
&\frac{\left\langle T_{l_3 l_4}^{l_1 l_2}(L) T_{l_3' l_4'}^{l_1' l_2'}(L') \right\rangle}{(2L+1) \langle C_{l_1} \rangle \langle C_{l_2} \rangle \langle C_{l_3} \rangle \langle C_{l_4} \rangle} \\
=\ & \delta_{LL'} \left[\delta_{l_1' l_2' l_3' l_4'}^{l_1 l_2 l_3 l_4} + \delta_{l_3' l_4' l_1' l_2'}^{l_1 l_2 l_3 l_4} + (-1)^{l_1+l_2+l_3+l_4} \left(\delta_{l_2' l_1' l_4' l_3'}^{l_1 l_2 l_3 l_4} + \delta_{l_4' l_3' l_2' l_1'}^{l_1 l_2 l_3 l_4} \right) \right. \\
&\left. + (-1)^{l_1+l_2+L} \left(\delta_{l_2' l_1' l_3' l_4'}^{l_1 l_2 l_3 l_4} + \delta_{l_4' l_3' l_1' l_2'}^{l_1 l_2 l_3 l_4} \right) + (-1)^{l_3+l_4+L} \left(\delta_{l_1' l_2' l_4' l_3'}^{l_1 l_2 l_3 l_4} + \delta_{l_3' l_4' l_2' l_1'}^{l_1 l_2 l_3 l_4} \right) \right], \qquad (3.33)
\end{aligned}$$

where $\delta_{l_1 l_2 l_3 l_4}^{l_1' l_2' l_3' l_4'} \equiv \delta_{l_1 l_1'} \delta_{l_2 l_2'} \delta_{l_3 l_3'} \delta_{l_4 l_4'}$, and so on. Using parity invariance, $l_1 + l_2 + L =$ even and $l_3 + l_4 + L =$ even, we find the covariance matrix diagonal. Thus, the diagonal terms for $L \neq 0$ and $l_1 \le l_2 < l_3 \le l_4$ are simplified very much as

$$\left\langle \left[T_{l_3 l_4}^{l_1 l_2}(L) \right]^2 \right\rangle = (2L+1) \langle C_{l_1} \rangle \langle C_{l_2} \rangle \langle C_{l_3} \rangle \langle C_{l_4} \rangle \left(1 + \delta_{l_1 l_2} + \delta_{l_3 l_4} + \delta_{l_1 l_2} \delta_{l_3 l_4}\right). \qquad (3.34)$$

This result is strictly correct only on the full sky; the incomplete sky makes the variance distribution much more scattered. Figure 3.6 plots the variance on the full sky as well as on the incomplete sky.

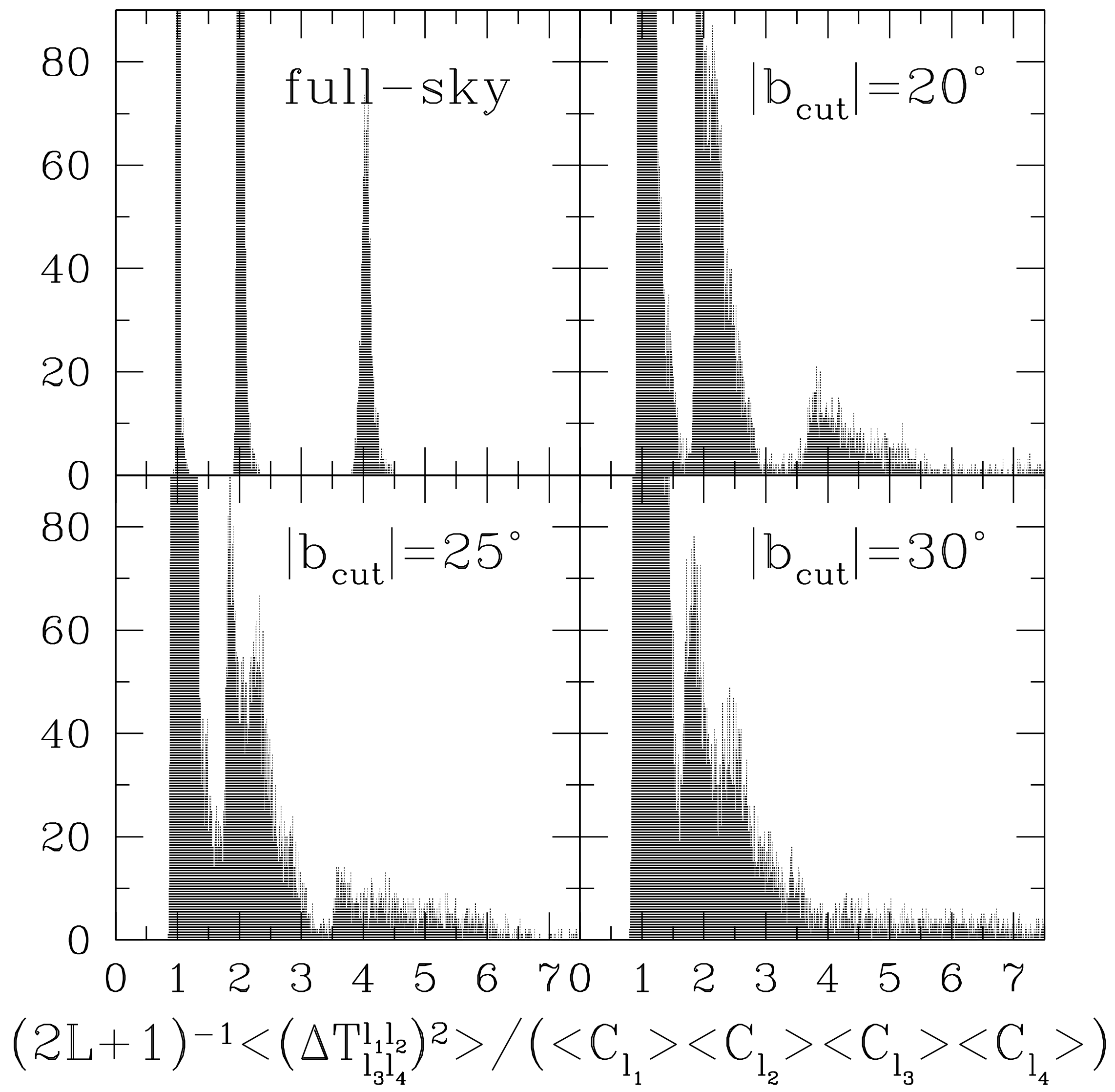

Figure 3.6: Variance of Angular Trispectrum I

Histograms of variance of the angular trispectrum for $L \neq 0$ and $l_1 \leq l_2 < l_3 \leq l_4$, for which the unconnected terms vanish on the full sky. There are 16,554 modes, up to a maximum multipole of 20. The meaning of the panels is the same as in figure 3.4.

For the rest of configurations for which the unconnected terms vanish, $L \neq 0$, $l_2 = l_3$, and $l_1 \neq l_4$, the covariance matrix is no longer diagonal in L, L' (Hu, 2001). Figure 3.7 plots the numerically evaluated variance on the full sky as well as on the incomplete sky. The variance divided by $(2L+1)\langle C_{l_1}\rangle\langle C_{l_2}\rangle\langle C_{l_3}\rangle\langle C_{l_4}\rangle$ is no longer an integer, but more scattered than that for $L \neq 0$ and $l_1 \leq l_2 < l_3 \leq l_4$ even on the full sky.

3.5 Power Spectrum and Bispectrum on the Incomplete Sky

Incomplete sky coverage destroys orthonormality of the spherical harmonics on the sky. The degree to which orthonormality is broken is often characterized by the coupling integral (Peebles, 1980),

$$W_{ll'mm'} \equiv \int d^2\hat{\mathbf{n}}\; W(\hat{\mathbf{n}}) Y^*_{lm}(\hat{\mathbf{n}})\, Y_{l'm'}(\hat{\mathbf{n}}) = \int_{\Omega_{\rm obs}} d^2\hat{\mathbf{n}}\; Y^*_{lm}(\hat{\mathbf{n}})\, Y_{l'm'}(\hat{\mathbf{n}}), \tag{3.35}$$

where $W(\hat{\mathbf{n}})$ is zero in a cut region otherwise 1, and $\Omega_{\rm obs}$ denotes a solid angle of the observed sky. When $W_{ll'mm'} \neq \delta_{ll'}\delta_{mm'}$, the measured harmonic transform of the temperature anisotropy field, a_{lm}, becomes a *biased* estimator of the true harmonic transform, $a^{\rm true}_{lm}$, through

$$a_{lm} = \sum_{l'=0}^{\infty} \sum_{m'=-l'}^{l'} a^{\rm true}_{l'm'} W_{ll'mm'}. \tag{3.36}$$

Hence, we must correct our estimators of the power spectrum and the bispectrum for the bias arising from incomplete sky coverage.

First, we derive a relationship between the angular power spectrum on the incomplete sky and that on the full sky. Taking the ensemble average of the estimator of the power spectrum, the pseudo-C_l (Wandelt et al., 1998, 2000), $C_l = (2l+1)^{-1}\sum_m |a_{lm}|^2$, we have

$$\begin{aligned}
\langle C_l \rangle &= \frac{1}{2l+1}\sum_{l'} C^{\rm true}_{l'} \sum_{mm'} |W_{ll'mm'}|^2 \\
&\approx \frac{1}{2l+1} C^{\rm true}_{l} \sum_{m}\sum_{l'm'} \int d^2\hat{\mathbf{n}}\; W(\hat{\mathbf{n}}) Y^*_{lm}(\hat{\mathbf{n}})\, Y_{l'm'}(\hat{\mathbf{n}}) \int d^2\hat{\mathbf{m}}\; W(\hat{\mathbf{m}}) Y_{lm}(\hat{\mathbf{m}})\, Y^*_{l'm'}(\hat{\mathbf{m}}) \\
&= \frac{1}{2l+1} C^{\rm true}_{l} \sum_{m} \int d^2\hat{\mathbf{n}}\; W(\hat{\mathbf{n}}) Y^*_{lm}(\hat{\mathbf{n}}) \int d^2\hat{\mathbf{m}}\; W(\hat{\mathbf{m}}) Y_{lm}(\hat{\mathbf{m}})\, \delta^{(2)}(\hat{\mathbf{n}} - \hat{\mathbf{m}}) \\
&= C^{\rm true}_{l} \int \frac{d^2\hat{\mathbf{n}}}{4\pi}\, W(\hat{\mathbf{n}}) P_l(1) \\
&= C^{\rm true}_{l} \frac{\Omega_{\rm obs}}{4\pi}.
\end{aligned} \tag{3.37}$$

In the second equality, we have taken $C^{\rm true}_{l'}$ out of the summation over l', as $|W_{ll'mm'}|^2$ peaks very sharply at $l = l'$, and $C^{\rm true}_{l'}$ varies much more slowly than $|W_{ll'mm'}|^2$ in l'. This approximation is good for nearly full sky coverage. In the third equality, we have used $\sum_{l'm'} Y_{l'm'}(\hat{\mathbf{n}})\, Y^*_{l'm'}(\hat{\mathbf{m}}) = \delta^{(2)}(\hat{\mathbf{n}} - \hat{\mathbf{m}})$. In the forth equality, we have used $\sum_m Y^*_{lm}(\hat{\mathbf{n}})\, Y_{lm}(\hat{\mathbf{m}}) = \frac{2l+1}{4\pi} P_l(\hat{\mathbf{n}} \cdot \hat{\mathbf{m}})$. The result indicates that the bias amounts approximately to a fraction of the sky covered by observations.

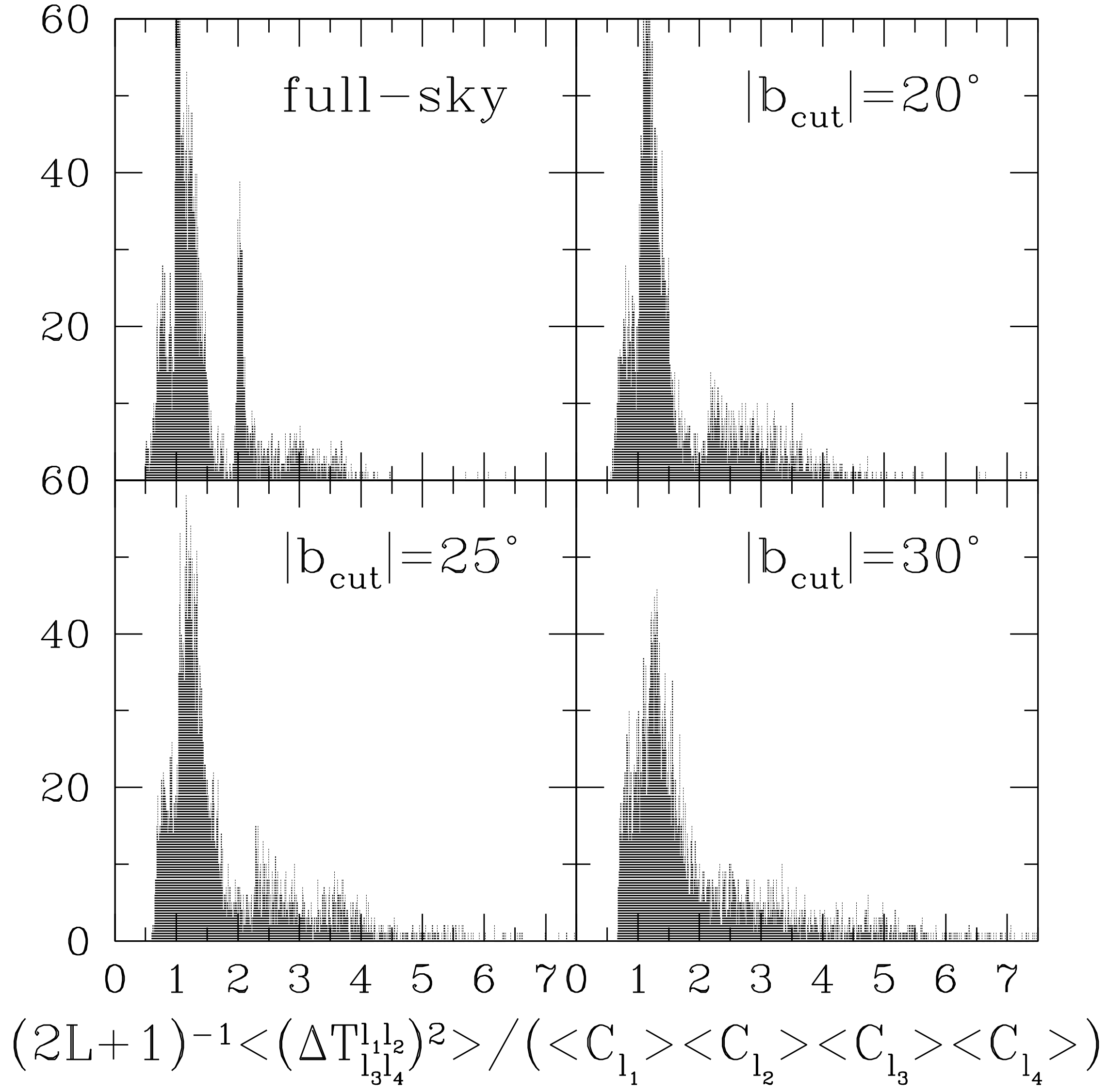

Figure 3.7: Variance of Angular Trispectrum II

Histograms of variance of the angular trispectrum for $L \neq 0$, $l_2 = l_3$, and $l_1 \neq l_4$, for which the unconnected terms vanish on the full sky. There are 4,059 modes, up to a maximum multipole of 20. The meaning of the panels is the same as in figure 3.4.

Next, we derive a relationship between the angular bispectrum on the incomplete sky and that on the full sky. We begin with

$$\langle a_{l_1m_1}a_{l_2m_2}a_{l_3m_3}\rangle = \sum_{\text{all } l'm'} \left\langle a^{\text{true}}_{l'_1m'_1}a^{\text{true}}_{l'_2m'_2}a^{\text{true}}_{l'_3m'_3}\right\rangle W_{l_1l'_1m_1m'_1}W_{l_2l'_2m_2m'_2}W_{l_3l'_3m_3m'_3}. \tag{3.38}$$

Rotational and parity invariance of the bispectrum implies the bispectrum given by

$$\langle a_{l_1m_1}a_{l_2m_2}a_{l_3m_3}\rangle = b_{l_1l_2l_3}\int d^2\hat{\mathbf{n}}\, Y^*_{l_1m_1}(\hat{\mathbf{n}})\,Y^*_{l_2m_2}(\hat{\mathbf{n}})\,Y^*_{l_3m_3}(\hat{\mathbf{n}}), \tag{3.39}$$

where $b_{l_1l_2l_3}$ is an arbitrary real symmetric function, which is related to the angular averaged bispectrum, $B_{l_1l_2l_3}$. When $b^{\text{true}}_{l_1l_2l_3}$ varies much more slowly than the coupling integral, we obtain

$$\begin{aligned}
\langle a_{l_1m_1}a_{l_2m_2}a_{l_3m_3}\rangle &= \sum_{\text{all } l'} b^{\text{true}}_{l'_1l'_2l'_3}\sum_{\text{all } m'}\int d^2\hat{\mathbf{n}}\, Y^*_{l'_1m'_1}(\hat{\mathbf{n}})\,Y^*_{l'_2m'_2}(\hat{\mathbf{n}})\,Y^*_{l'_3m'_3}(\hat{\mathbf{n}}) \\
&\quad\times\int d^2\hat{\mathbf{n}}_1\, W(\hat{\mathbf{n}}_1)Y_{l'_1m'_1}(\hat{\mathbf{n}}_1)\,Y^*_{l_1m_1}(\hat{\mathbf{n}}_1) \\
&\quad\times\int d^2\hat{\mathbf{n}}_2\, W(\hat{\mathbf{n}}_2)Y_{l'_2m'_2}(\hat{\mathbf{n}}_2)\,Y^*_{l_2m_2}(\hat{\mathbf{n}}_2) \\
&\quad\times\int d^2\hat{\mathbf{n}}_3\, W(\hat{\mathbf{n}}_3)Y_{l'_3m'_3}(\hat{\mathbf{n}}_3)\,Y^*_{l_3m_3}(\hat{\mathbf{n}}_3) \\
&\approx b^{\text{true}}_{l_1l_2l_3}\int d^2\hat{\mathbf{n}}\, W(\hat{\mathbf{n}})Y^*_{l_1m_1}(\hat{\mathbf{n}})\,Y^*_{l_2m_2}(\hat{\mathbf{n}})\,Y^*_{l_3m_3}(\hat{\mathbf{n}}).
\end{aligned} \tag{3.40}$$

Then, we calculate the angular averaged bispectrum, $B_{l_1l_2l_3}$ (Eq.(3.15)). By convolving equation (3.18) with the Wigner-$3j$ symbol and using the identity (3.19), we obtain

$$\begin{aligned}
\langle B_{l_1l_2l_3}\rangle &\approx b^{\text{true}}_{l_1l_2l_3}\sqrt{\frac{4\pi}{(2l_1+1)(2l_2+1)(2l_3+1)}}\begin{pmatrix} l_1 & l_2 & l_3 \\ 0 & 0 & 0\end{pmatrix}^{-1} \\
&\quad\times\sum_{\text{all } m}\int d^2\hat{\mathbf{m}}\, Y_{l_1m_1}(\hat{\mathbf{m}})\,Y_{l_2m_2}(\hat{\mathbf{m}})\,Y_{l_3m_3}(\hat{\mathbf{m}}) \\
&\quad\times\int d^2\hat{\mathbf{n}}\, W(\hat{\mathbf{n}})Y^*_{l_1m_1}(\hat{\mathbf{n}})\,Y^*_{l_2m_2}(\hat{\mathbf{n}})\,Y^*_{l_3m_3}(\hat{\mathbf{n}}) \\
&= b^{\text{true}}_{l_1l_2l_3}\sqrt{\frac{(2l_1+1)(2l_2+1)(2l_3+1)}{4\pi}}\begin{pmatrix} l_1 & l_2 & l_3 \\ 0 & 0 & 0\end{pmatrix}^{-1} \\
&\quad\times\int\frac{d^2\hat{\mathbf{m}}}{4\pi}\int\frac{d^2\hat{\mathbf{n}}}{4\pi}\, W(\hat{\mathbf{n}})P_{l_1}(\hat{\mathbf{m}}\cdot\hat{\mathbf{n}})\,P_{l_2}(\hat{\mathbf{m}}\cdot\hat{\mathbf{n}})\,P_{l_3}(\hat{\mathbf{m}}\cdot\hat{\mathbf{n}}) \\
&= b^{\text{true}}_{l_1l_2l_3}\sqrt{\frac{(2l_1+1)(2l_2+1)(2l_3+1)}{4\pi}}\begin{pmatrix} l_1 & l_2 & l_3 \\ 0 & 0 & 0\end{pmatrix}\frac{\Omega_{\text{obs}}}{4\pi} \\
&= B^{\text{true}}_{l_1l_2l_3}\frac{\Omega_{\text{obs}}}{4\pi},
\end{aligned} \tag{3.41}$$

where we have used the identity,

$$\int_{-1}^{1}\frac{dx}{2}\,P_{l_1}(x)P_{l_2}(x)P_{l_3}(x) = \begin{pmatrix} l_1 & l_2 & l_3 \\ 0 & 0 & 0\end{pmatrix}^2. \tag{3.42}$$

Thus, the bias for the angular bispectrum on the incomplete sky is also approximately given by a fraction of the sky covered by observations.